MICROSTRUCTURAL CHARACTERISATION OF AS-DEPOSITED AND REHEATED WELD METAL – HIGH STRENGTH STEEL WELD METALS




E. Keehan **L. Karlsson** **M. Thuvander** **E. Bergquist**

ESAB AB, Gothenburg (Sweden)

ABSTRACT

The problems encountered with the interpretation of martensite and the various forms of bainite that are found in high strength steel weld metals have been addressed. Field emission gun scanning electron microscopy was found to overcome resolution difficulties often met with light optical microscopy and conventional scanning electron microscopy. Microstructural constituents were characterised both in the as-deposited and reheated tempered states. The characterisation of retained austenite and identification of carbide types remains challenging, and transmission electron microscopy is required.

IIW-Thesaurus keywords: *Austenite; Bainite; Electron microscopes; High strength steels; Martensite; Measuring instruments; Microscopes; Microstructure; Steels, Weld metal.*

1 INTRODUCTION

For many decades, the interpretation of high strength steel and weld metal microstructural constituents such as upper and lower bainite along with martensite has been a challenging task for metallurgists. All three microstructural constituents generally have fine scale morphology, and it is very difficult to differentiate between them with light optical microscopy (LOM) and conventional scanning electron microscopy (SEM). The visual microstructural difference between martensite, lower and upper bainite is basically whether or not carbide forms, and if so, where it forms. Figure 1 presents a schematic diagram of the formation of upper and lower bainite from literature [1] along with that of martensite.

Recently, in addition to the classical constituents of martensite, lower and upper bainite, a novel form of bainite – coalesced bainite – was found to develop in some high strength steel weld metals [2]. Coalesced bainite was found to form in particular at compositions where the martensite start temperature (M_S) and the bainite start temperature (B_S) are close to each other. It can develop to have a large grain size and is believed to be negative for mechanical properties, particularly impact toughness. A schematic diagram of its formation mechanism is presented in Figure 2 [3]. The presence of and the amount of martensite, upper, lower and coalesced bainite largely determines both the strength and toughness of a high strength steel weld metal.

In combination with LOM and SEM, it has been common practice to use hardness testing to complement and support interpretations. When resources are available, transmission electron microscopy (TEM) is often used, however this is a time consuming characterisation method with the area analysed limited to a small region. In the past decade, field emission gun scanning electron microscopy (FEGSEM) has become more commonly used in material science, and it offers many advantages. Greater resolution than conventional SEM is obtained and carbides in the order of a few nanometers are possible to image. In addition, FEGSEM offers greater flex-

Doc. IIW-1782-06 (ex-doc. IX-2187-06/IX-J-0102-06) recommended for publication by Commission IX “Behaviour of metals subjected to welding”.

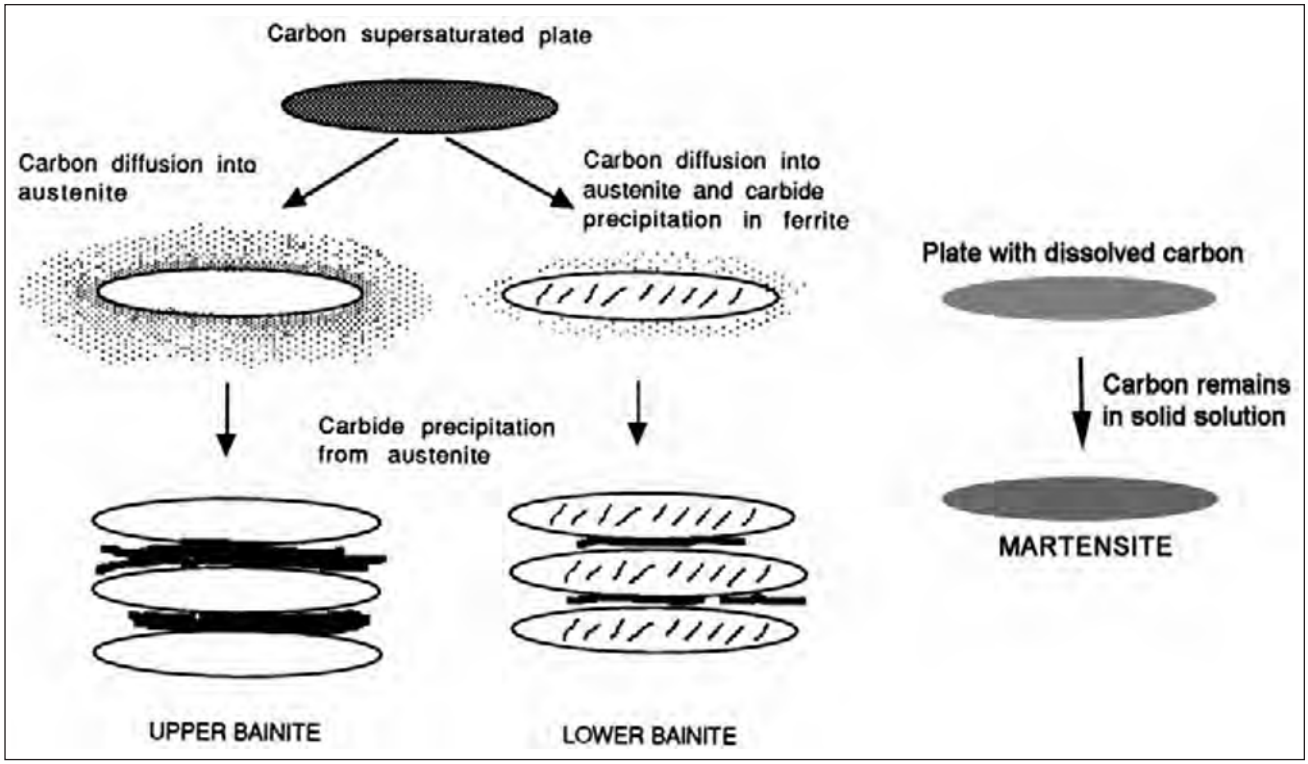

Figure 1 – Schematic diagram of the formation of upper and lower bainite [1] along with martensite

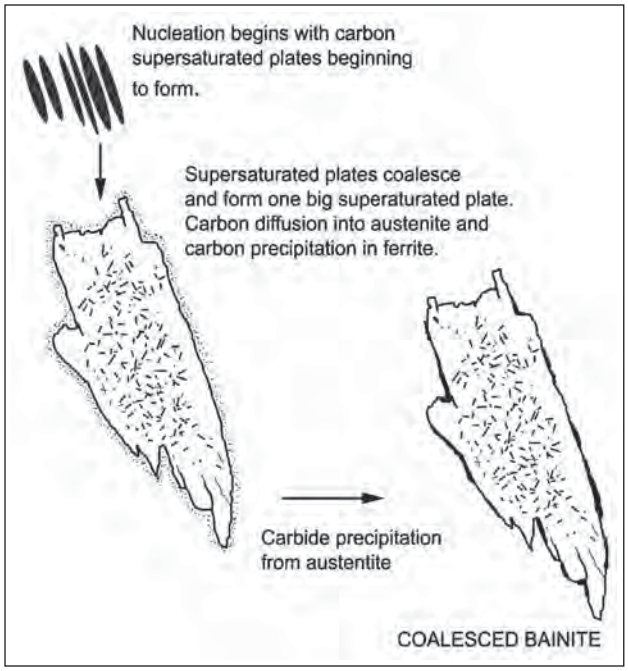

Figure 2 – Schematic diagram of the formation of coalesced bainite [3]

ibility to examine many areas with high resolution in a limited time in comparison to TEM. This document presents microscopy results with a focus on FEGSEM investigations showing martensite, upper, lower and coalesced bainite from various weld metals studied in a large research project [4]. The changes in morphology as a result of reheating due to multiple weld passes within the joint are also presented.

2 EXPERIMENTAL DETAILS

All welded joints were made according to ISO 2560 using 20 mm plates with a backing strip. The joints were buttered prior to the deposition of the experimental weld metals that took place in 33 cm runs with two or three runs per layer using shielded metal arc welding (SMAW). Table 1 presents the compositional range of the weld metals studied. A range of heat inputs and interpass temperatures were used that gave various cooling rates. Since composition and cooling rate play an important role in determining what microstructural constituent develops, the exact level of the more important alloy

Table 1 – Composition range in wt. %, unless otherwise stated, of the weld metals studied

C	Ni	Mn	Cr	Mo	Si
0.03 – 0.34	3.0 – 10.5	0.5 – 2.2	0.1 – 1.4	0.4 – 0.6	0.2 – 0.4
P	**Cu**	**S**	**O / ppm**	**N / ppm**	**V**
0.01 – 0.02	0.01 – 0.30	0.01	260 – 380	100 – 260	0.016 – 0.021

elements and the $t_{8/5}$ (estimated cooling time between 800 and 500 °C calculated from WeldCalc [5]) is stated where important.

Specimens from the weld metal cross section, extracted perpendicular to the welding direction were mounted in bakelite, wet ground and polished to 1 µm diamond solution. The specimens were etched using 2 % nital or Kalling 1 etchants, for analysis with light optical microscopy (LOM) and field emission gun scanning electron microscopy (FEGSEM). A Leitz Aristomet light optical microscope and a Leo Ultra 55 FEGSEM were used in these examinations. For TEM studies, 3 mm disc shape samples, extracted perpendicular to the welding direction, were ground to between 50 and 80 µm in thickness, and then jet electropolished at –35 °C using 10 % perchloric acid in methanol. After electropolishing the specimens were further thinned by ion beam milling for a few minutes at a low angle using a Gatan Precision Ion Polishing System (PIPS). These specimens were examined with a Jeol 2000 FX.

3 MICROSTRUCTURAL CONSTITUENTS

Figure 3 presents two typical LOM micrographs showing martensite, upper, lower and coalesced bainite in as-deposited last beads in two different welded joints. From these micrographs, it is difficult to interpret the microstructural constituents due to the limited resolution obtained with LOM. Further knowledge at higher magnifications is required to identify constituents with certainty. The typical morphology of each microstructural constituent will now be presented using electron microscopy.

3.1 Upper bainite

Figure 4 presents a micrograph showing the typical appearance of upper bainite using FEGSEM. The micrograph was recorded in the as-deposited last bead of a welded joint with 0.05 C, 3.1 Ni, 2.0 Mn, 0.4 Cr, 0.6 Mo deposited with welding parameters that gave $t_{8/5}$ equal to 19 seconds approximately. It is observed that very often the laths are separated from each other with cementite and/or retained austenite at the lath boundaries. Using FEGSEM it is difficult to differentiate between cementite and retained austenite just from imaging, and crystallographic information is required. It may be possible to acquire information on the crystallography using an Electron Backscattered Diffraction (EBSB) detector, which is an attachment to the FEGSEM, but this is a challenging task due to resolution. Similar problems arise with the characterisation of carbides.

Figure 4 can be compared with Figure 5 where the morphology of tempered upper bainite is shown. The micrograph (Figure 5) was taken in an underlying reheated bead of the same welded joint where upper bainite was characterised in Figure 4. Within the micrograph it is seen that the cementite and precipitates have become more spheroidised as a result of reheating.

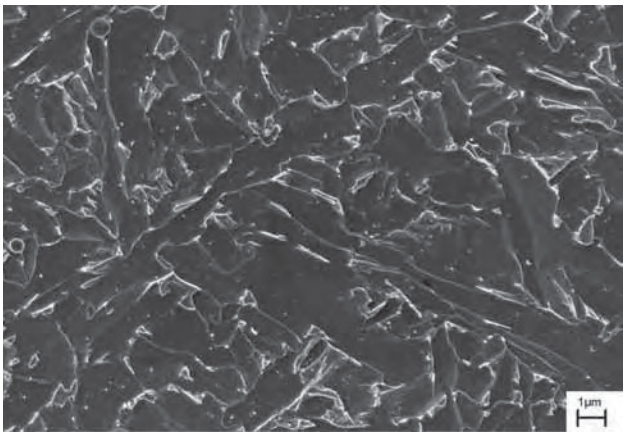

The weld metal contained 0.05 C, 3 Ni, 2 Mn, 0.5 Cr, 0.6 Mo and had $t_{8/5}$ = 19 s approximately.

Figure 4 – FEGSEM micrograph showing upper bainite in an as-deposited last bead

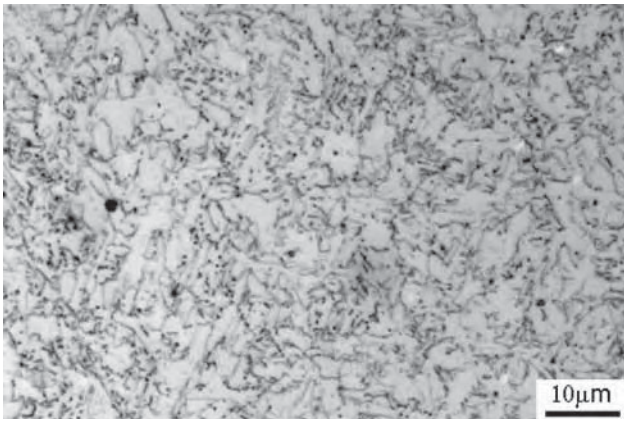

a) As-deposited weld metal containing 0.05 C, 3.1 Ni, 2.0 Mn, 0.4 Cr, 0.6 Mo and $t_{8/5}$ = 19 s

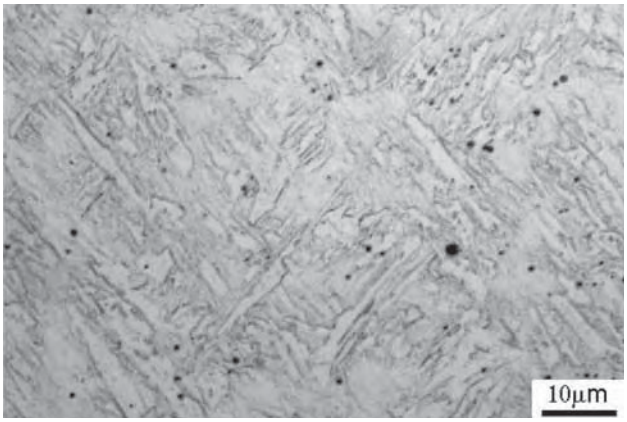

b) As-deposited weld metal containing 0.03 C, 6.5 Ni, 2.2 Mn, 0.4 Cr, 0.6 Mo with $t_{8/5}$ = 11 s

At this resolution, it is difficult to distinguish between martensite, upper, lower and coalesced bainite without having prior knowledge at higher resolution.

Figure 3 – Two LOM micrographs that show different forms of bainite and martensite between them

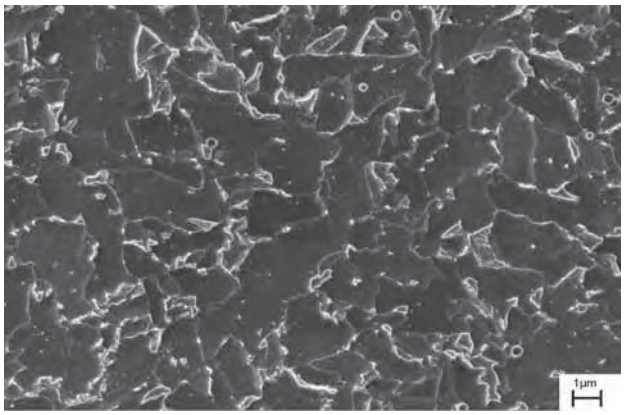

The weld metal contained 0.05 C, 3.0 Ni, 2.0 Mn, 0.5 Cr, 0.6 Mo and had $t_{8/5}$ = 19 s.

Figure 5 – Tempered upper bainite in the centre of a reheated bead shown using FEGSEM

3.2 Lower bainite

Figure 6 presents the typical morphology of lower bainite using FEGSEM in a weld metal containing 0.11 C, 7.0 Ni and 0.5 Mn, 0.1 Cr, 0.4 Mo welded with parameters giving $t_{8/5}$ equal to 10 seconds. It is observed that precipitation also takes place within the ferrite laths as well as at the lath boundaries. Lower bainite develops at lower austenite transformation temperatures and often at faster cooling rates in comparison to upper bainite. As a result, the mobility of carbon is reduced which leads to the precipitation also within the laths.

The morphology of tempered lower bainite is shown with FEGSEM in Figure 7. The micrograph was taken in a reheated underlying bead in a weld metal containing 0.11 C, 7.0 Ni and 0.5 Mn, 0.1 Cr, 0.4 Mo and welding parameters that gave $t_{8/5}$ = 10 s. In the tempered condition, it was found that the precipitates both within the laths and at the lath boundaries had coarsened and spheroidised as a result of the reheating.

3.3 Coalesced bainite

A micrograph showing coalesced bainite in an as-deposited last bead is presented in Figure 8. The micro-

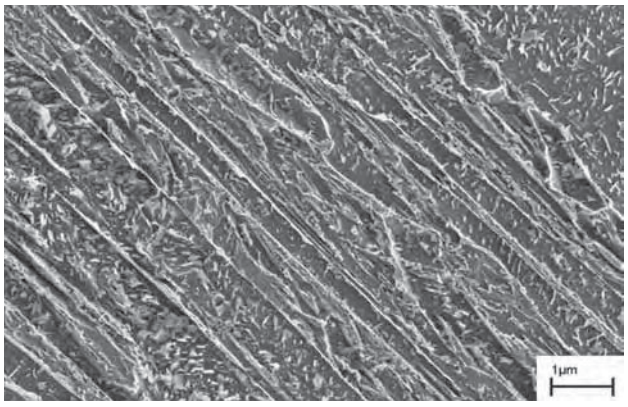

Figure 6 – Lower bainite shown using FEGSEM, in as-deposited weld metal containing 0.18 C, 6.9 Ni, 0.6 Mn and 0.4 Mo along with welding parameters that gave $t_{8/5}$ = 10 s

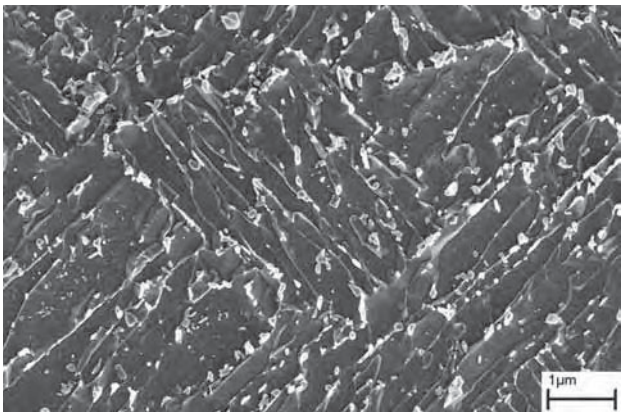

The micrograph was recorded on a weld metal containing 0.11 C, 7.0 Ni and 0.5 Mn, 0.1 Cr, 0.4 Mo and welding parameters that gave $t_{8/5}$ = 10 s.

Figure 7 – Tempered lower bainite in the centre of a reheated bead shown using FEGSEM

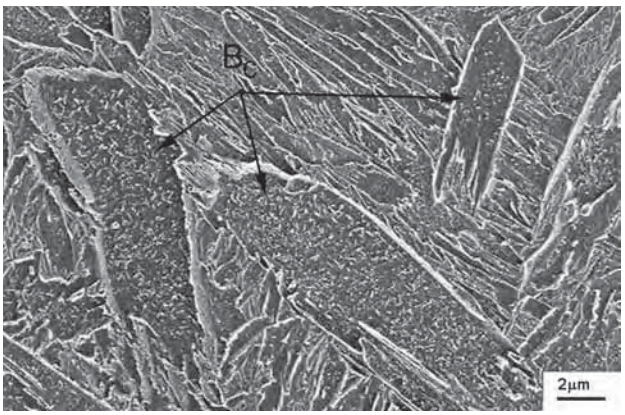

Figure 8 – A FEGSEM micrograph showing coalesced bainite (B_c) in as-deposited weld metal containing 0.08 C, 10.5 Ni, 0.6 Mn 1.1 Cr, 0.3 Mo and $t_{8/5}$ = 9 s

graph was recorded in a weld metal containing 0.08 C, 10.5 Ni, 0.6 Mn 1.1 Cr, 0.3 Mo and had a $t_{8/5}$ = 9 s. The weld metal composition was chosen with the aim of giving M_S and B_S close to each other in order to produce large quantities of coalesced bainite for the purpose of its characterisation. The coalescence of many bainitic ferrite plates giving one large grain is clearly seen in the lower part of the top right coalesced grain. Numerous precipitates developed within the grain, and this is to be expected since the relatively large grain forms at low transformation temperature where carbon mobility is not so great. Some carbide is also found to have developed at the grain boundaries.

Tempered coalesced bainite is shown in Figure 9. The image was taken in a reheated bead of the same welded joint used to capture coalesced bainite in the as-deposited state (Figure 8). A higher magnification image showing the carbides within the grain is presented in Figure 10.

3.4 Martensite

Martensite is shown in Figure 11 using FEGSEM. The micrograph was captured in the last bead of a welded

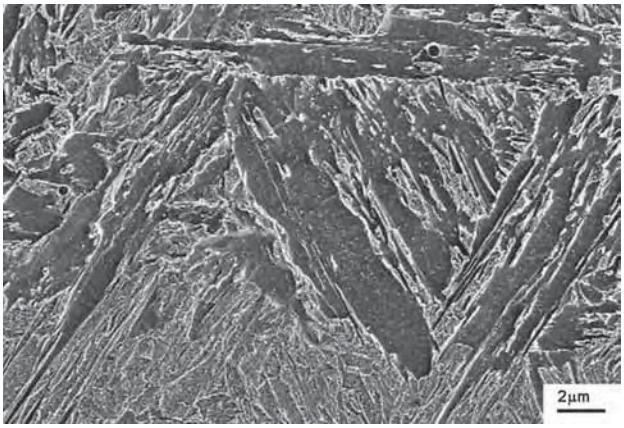

Figure 9 – Tempered coalesced bainite shown with FEGSEM in weld metal containing 0.08 C, 10.5 Ni, 0.6 Mn, 1.1 Cr, 0.3 Mo and $t_{8/5}$ = 9 s

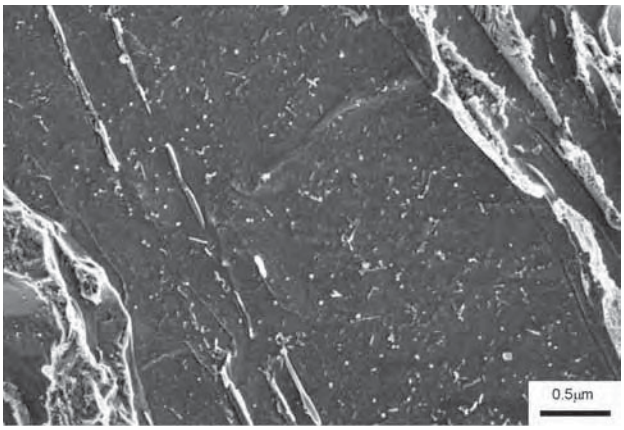

Figure 10 – A high magnification micrograph showing the precipitates that have spheroidised within the tempered coalesced bainite grain shown in Figure 9 – 0.08 C, 10.5 Ni, 0.6 Mn 1.1 Cr, 0.3 Mo and $t_{8/5}$ = 9 s

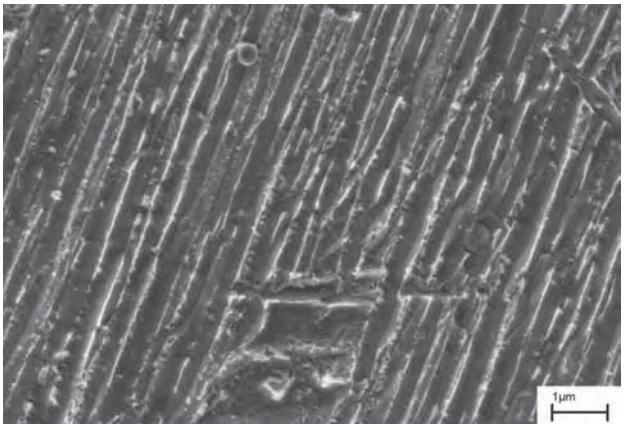

Figure 11 – Martensite shown using FEGSEM, in the last bead of a weld metal containing 0.08 C, 1.5 Mn, 0.4 Mo with $t_{8/5}$ = 1 s

joint containing 0.08 C, 1.5 Mn, 0.4 Mo which had a cooling rate giving $t_{8/5}$ = 1 s. It can form at fast cooling rates, or when austenite is stabilised to low transformation temperatures through alloying. Martensite is a hard and strong constituent as a result of carbon remaining in solid solution within the matrix and the high dislocation density generated from the inhomogeneous shear transformation mechanism.

Upon tempering, martensite decomposes, and carbon begins to form precipitates. Depending on carbon content different amounts of precipitates form. Two FEGSEM images of tempered martensite showing the effect of carbon content are presented in Figures 12 and 13. Figure 12 shows an underlying reheated bead with composition containing 0.032 C, 7.2 Ni, 2.0 Mn, 0.5 Cr and 0.6 Mo with $t_{8/5}$ = 12 s while Figure 13 shows a reheated bead with 0.34 C, 6.9 Ni, 0.6 Mn, 0.1 Cr and 0.4 Mo with $t_{8/5}$ = 10 s.

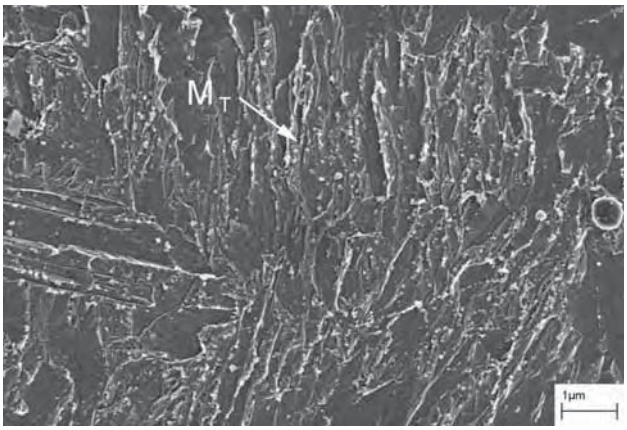

Figure 12 – Tempered martensite (M_T) in the centre of a reheated bead containing 0.032 C, 7.2 Ni, 2.0 Mn, 0.5 Cr and 0.6 Mo with $t_{8/5}$ = 12 s shown using FEGSEM

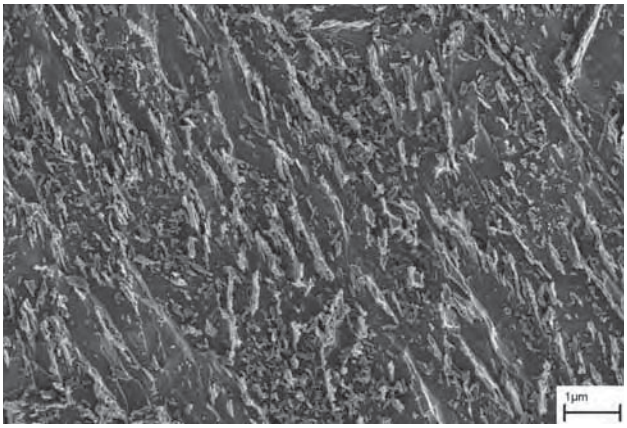

Figure 13 – Tempered martensite in the centre of a reheated bead containing 0.34 C, 6.9 Ni, 0.6 Mn, 0.1 Cr and 0.4 Mo with $t_{8/5}$ = 10 s shown using FEGSEM

3.5 Retained austenite

Retained austenite is often found to be present in small amounts in high strength steel weld metal microstructures. It arises from the incomplete transformation of austenite and is mainly located in the as-deposited last bead since it normally decomposes once reheating takes place. It may arise due to a high alloying content that stabilises austenite to low transformation temperatures. The presence of retained austenite is generally undesirable in large amounts and causes a loss of strength and toughness.

It is difficult to identify retained austenite with certainty using scanning electron microscopy. It can be charac-

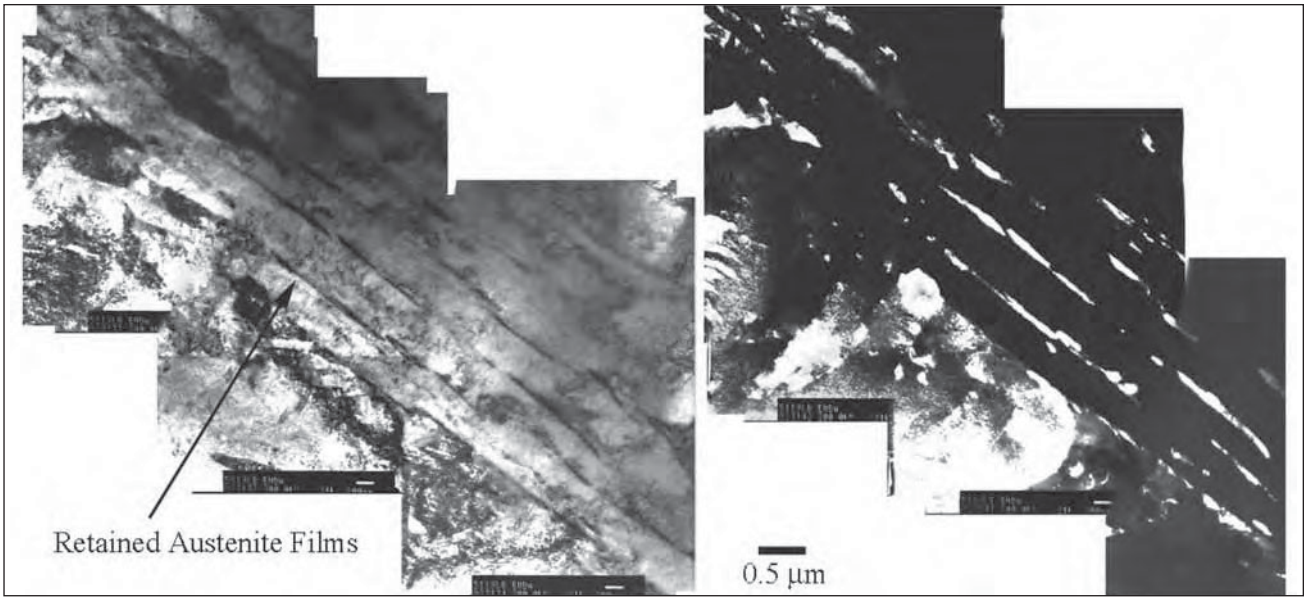

Figure 14 – TEM bright field (Left) and dark field (Right) images showing thin films of retained austenite in as-deposited weld metal containing 0.03 C, 9.2 Ni and 2.1 Mn, 0.5 Cr, 0.4 Mo along with a cooling rate giving $t_{8/5}$ = 11 s

terised using electron diffraction with TEM or with X-ray diffraction. Figure 14 shows a bright field image (left image) with corresponding dark field image (right image) taken in as-deposited weld metal containing 0.03 C, 9.2 Ni and 2.1 Mn, 0.5 Cr, 0.4 Mo along with a cooling rate giving $t_{8/5}$ = 11 s. The dark field image was formed using an austenite reflection in a diffraction pattern. It is clearly seen that the black films between the martensitic laths in the bright field image appear bright in the dark field.

4 CONCLUSIONS

FEGSEM, which offers much greater resolution than LOM, is an excellent tool for the characterisation of high strength steel microstructures such as martensite, upper, lower, and coalesced bainite.

The characterisation of retained austenite and carbides is difficult with FEGSEM since crystallographic information is required. Depending on the carbide size or film thickness, characterisation of these constituents may be possible with FEGSEM in combination with EBSD, however this is challenging. TEM offers no such limitations, and retained austenite along with carbides of all sizes and forms can be characterised.

The microstructure in reheated beads is often very difficult to interpret due to the complex morphology obtained after reheating. An understanding of the microstructure in the as-deposited last bead eases these difficulties.

REFERENCES

[1] Takahashi M., Bhadeshia H.K.D.H.: A model for the transition from upper to lower bainite, Materials Science and Technology, 1990, 6, pp. 592-603.

[2] Keehan E., Microstructure characterisation of a high strength steel weld metal containing the novel constituent coalesced bainite, Ph. D. thesis, Chalmers University of Technology, Effect of microstructure on mechanical properties of high strength steel weld metals, Paper 3, 2004.

[3] Keehan E. *et al.*: Microstructure and properties of novel high strength steel weld metals, Doc. IIW-1703-05 (ex-doc. IX-2146-05), Welding in the World, 2005, Vol. 49, No. 9/10, pp. 19-31.

[4] Keehan E., Effect of microstructure on mechanical properties of high strength steel weld metals, in Experimental Physics, 2004, Chalmers University of Technology: Gothenburg, Sweden.

[5] SSAB, WeldCalc. 1998-99: Oxelösund, Sweden.